Research on Polycrystalline Thin-Film CuInGaSe₂ Solar Cells

Annual Subcontract Report
3 May 1991 – 21 May 1993

W. S. Chen, J. M. Stewart,
R. A. Mickelsen, W. E. Devaney,
B. J. Stanbery
Boeing Defense & Space Group
Seattle, Washington

NREL technical monitor: H. S. Ullal

◆◇►NREL

MASTER

This publication was reproduced from the best available camera-ready copy
submitted by the subcontractor and received no editorial review at NREL.

NOTICE

Printed on recycled paper

DISCLAIMER

Portions of this document may be illegible
electronic image products. Images are
produced from the best available original
document.

PREFACE

Since 1976 The Boeing Company has conducted pioneering research and development of $CuInSe_2$ and $CuInGaSe_2$ polycrystalline thin film solar cells. We have consistently demonstrated state-of-the-art efficiency for these thin film solar cells. The results reported herein for our work in performance of this contract mark the end of that tradition of technology leadership at Boeing.

Fortunately, Boeing has effectively transferred much of the technology for high efficiency cell preparation to other research organizations. Given the very small worldwide resource base available for $CuInSe_2$ cell development, this technology transfer contribution is likely to be significant to the future, successful advancement of these attractive polycrystalline thin-film solar cells.

The authors would like to acknowledge the critical contributions of Richard Murray, Rex Armstrong and Dan Peterson to this work. Each and together they have provided the infrastructure for and much of the execution of the work reported herein. We would also like to acknowledge Dr. Robert Burgess for his contributions to our understanding of the chemistry of the CBD process.

_____   7 June 1993
Approval Signature, Program Manager   Date

SUMMARY

OBJECTIVES

The objectives of this research effort were to fabricate high efficiency CdZnS/CuGaInSe$_2$ thin film solar cells, and to develop improved transparent conductor window layers such as ZnO. Our specific technical milestone for Phase I was the demonstration of an AM1.5 global 13%, 1cm^2 total area CuGaInSe$_2$ thin film solar cell; and for Phase II, the demonstration of an AM1.5 global 13.5%, 1cm^2 total area efficiency. In addition, we have delivered optimized CuGaInSe$_2$ solar cells and CuGaInSe$_2$ films on molybdenum-metallized substrates biannually.

DISCUSSION

Analysis of the properties of the best ZnO/CdZnS/CuInGaSe$_2$ cells developed by Boeing for SERI under a prior subcontract suggested that significant performance improvements could be realized by further optimization of the thin CdZnS layer to reduce shunt currents while maintaining subbandgap transparency, the ZnO layer to reduce IR absorption while maintaining adequate lateral conductivity, and the CuInGaSe$_2$ (CIGS) layer to optimize gallium content and gradients along with minority carrier transport properties.

During the early portion of this contract phase our activities were focused on three areas. First, our CIGS deposition system was modified to double its substrate capacity. This increased throughput has proven critical to speeding the pace of process development by providing multiple substrates from the same CIGS run which can be used to reduce uncertainty in the cause of differences resulting from the intentional variation of other process parameters. Second, new tooling was developed to enable investigation of a modified aqueous CdZnS process whose goal was to improve the yield of this critical step in the device fabrication process. Third, our ZnO sputtering system was upgraded to improve its reliability and reproducibility; a dual rotatable cathode metallic source was installed; and the sputtering parameters further optimized to improve ZnO's properties as a Transparent Conducting Oxide (TCO).

Continuous improvements in thermal and flux uniformity of the new CIGS deposition system substrate fixturing proceeded throughout this contract and sufficiently high temperatures for device-quality CIGS deposition were achieved. Optimization of the modified aqueous Cd$_{1-y}$Zn$_y$S process has enabled us to reproducibly deposit adherent, substantially pinhole-free films over a 2" x 2" substrate for zinc fractions in the range $0 \leq y \leq 0.30$. The electro-optical properties of the ZnO were improved, enabling the use of thinner layers while preserving high light-generated currents and fill factors.

CONCLUSIONS

Our best CIGS cell fabricated *prior* to this contract at Boeing was a ZnO/Cd$_{0.82}$Zn$_{0.18}$S/CuIn$_{0.72}$Ga$_{0.28}$Se$_2$ cell with an AM1.5 efficiency of 12.5%. Combining the refined CdZnS process with CIGS from the newly fixtured deposition system enabled us to fabricate and deliver a ZnO/Cd$_{0.80}$Zn$_{0.20}$S/CuIn$_{0.74}$Ga$_{0.26}$Se$_2$ cell on alumina whose I-V characteristics as measured by NREL under standard test conditions gave 13.7% efficiency with $V_{oc} = 0.5458$ volts, $J_{sc} = 36.34$ mA, FF = 0.6838 and a cell area of 0.9895 cm^2. This NREL measurement verifies that we have met our key contract technical milestone. Furthermore, our best $\cong 1$ cm^2 ZnO/Cd$_{0.76}$Zn$_{0.24}$S/CuIn$_{0.75}$Ga$_{0.25}$Se$_2$ cell on low-cost soda lime glass was delivered to NREL with $V_{oc} = 0.599$ volts, $J_{sc} = 35.48$ mA/cm^2, FF = 0.688 and efficiency of **14.6%**.

TABLE OF CONTENTS

LIST OF FIGURES

LIST OF TABLES

1.0 INTRODUCTION

This is the Final Technical Progress Report on our activities and achievements in performance of a research program entitled "Research on Polycrystalline Thin Film CuGaInSe$_2$ Solar Cells." The work reported herein was conducted in the period between May 3, 1991 and May 21, 1993. This work continues the research performed under several previous contracts and focuses on further development of thin film polycrystalline heteroface solar cells using the mixed alloy Copper Indium Gallium diSelenide (CIGS or CuIn$_{1-x}$Ga$_x$Se$_2$) as the p-type absorber layer and Cadmium Zinc Sulfide (Cd$_{1-y}$Zn$_y$S) mixed alloys as the n-type contact layer with an overlayer of ZnO transparent conducting oxide (TCO) for majority carrier collection to the grids. This ZnO/CdZnS/CuGaInSe$_2$ semiconductor structure is deposited sequently onto molybdenum coated alumina or glass substrates using evaporation, sputtering, and chemical bath deposition processes. The device is finished with a top grid structure composed of gridlines and buss bars and in some cases a MgF$_2$ antireflection coating. This cell structure is shown schematically in figure 1-1.

Our best cell fabricated at Boeing during Phase 1 of this contract had a 13.1% AM1.5 efficiency. This cell was fabricated on an alumina substrate using CIGS material with a 20% Ga content. During this second phase of our contract we improved the cell efficiency to 13.7% by reducing the optical losses, improving the quality of the CIGS material, and increasing the Ga content to 26%. Finally, cells with total area efficiencies over 14% and open circuit voltages exceeding 580 mV have been achieved by substituting inexpensive soda lime glass as the substrate material.
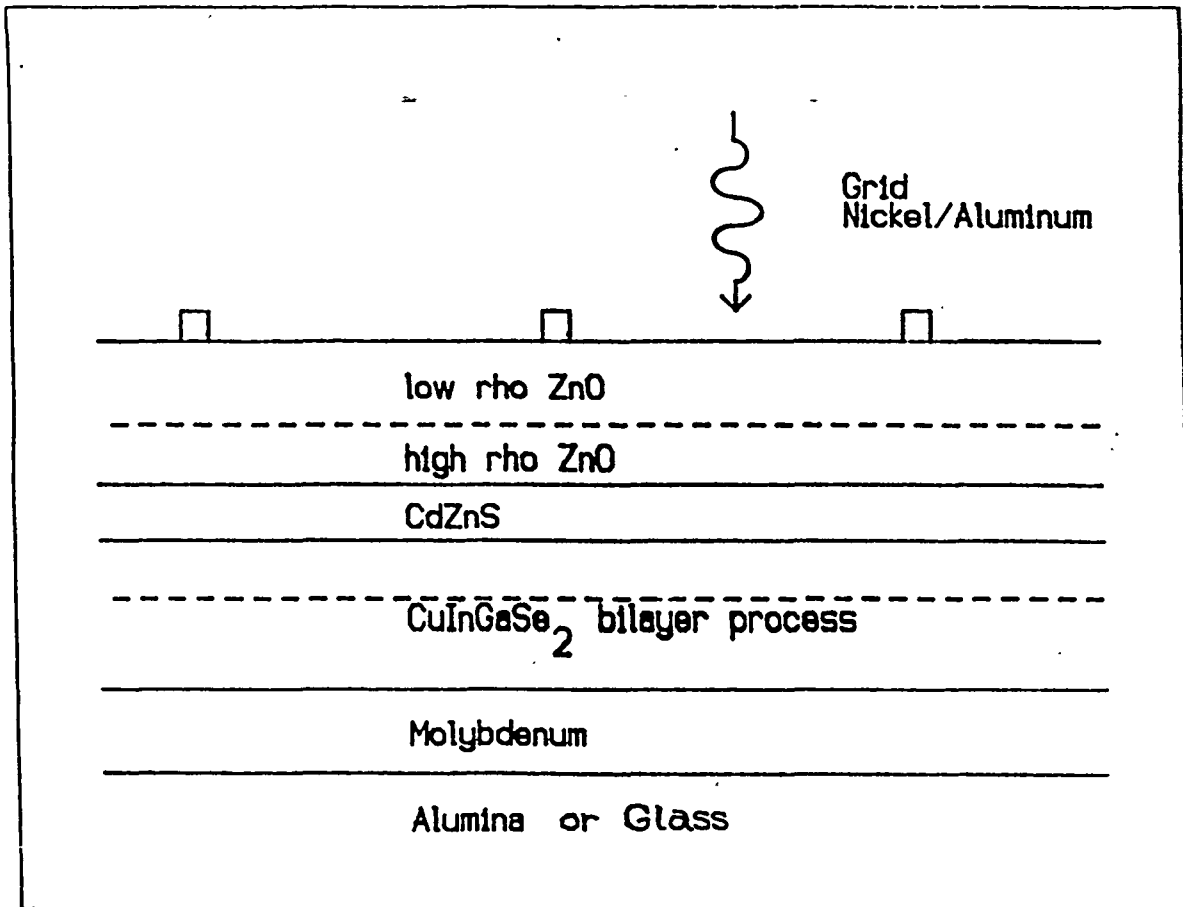
Figure 1-1. Structure of ZnO/CdZnS/CuInGaSe$_2$ solar cells

1

2.0   METHODS

2.1   CU(IN,GA)SE$_2$

Our baseline procedure for the preparation of CuGaInSe$_2$ (CIGS) films relies upon co-evaporation of the four elements onto heated molybdenum coated substrates [1]. EIES controllers are used to control the evaporation rate and film thickness for the Cu, In, and Ga vaporization sources while a quartz crystal unit is utilized for Se rate/thickness control. In order to ameliorate composition gradients resulting from spatially separated sources, the substrates (four, each 2" by 2" in size) are rotated. The substrate rotation also assists in reducing temperature gradients due to the nonuniformity of the heater lamp illumination. Deposition times of 40-50 minutes, excess Se evaporation rates, substrate temperatures of 450-700°C, and the Boeing two-layer deposition process where the Cu rate is adjusted, are all standard film preparation conditions. The vacuum system is evacuated with a liquid nitrogen trapped oil diffusion pump and the pressure during film deposition is approximately 10^{-6} millibar.

2.2   CDZNS CHEMICAL DEPOSITION

The chemical deposition of thin CdZnS film is essentially unchanged from previous work [2]. During this contract several refinements have been made. A new teflon sample holder which can accomodate up to four 2 x 2 inch samples has been made and used. Premixed solutions are prepared as follows:

(1) CdCl$_2$ solution

CdCl$_2$·2 ($^{1}/_{2}$) H$_2$O	(0.0084 M)	1.92 g
NH$_4$Cl	(0.026 M)	1.39 g
D.I. Water		1000 ml

(2) Thiourea solution

Thiourea	(0.0834 M)	6.35 g
D.I. Water		1000 ml

(3) ZnCl$_2$ solution

ZnCl$_2$	10.0 g
D.I. Water	400 ml

Add enough NH$_4$Cl to dissolve the white precipate, Zn(OH)$_2$, until the solution is clear.

(4) NH$_4$OH   (reagent 28%-30%)   50 ml

   D.I. Water   350 ml

Prepared solutions are stored separately and can be used for a long time.

A good film, even with Zn, can be deposited when the chemical reaction is slow. This condition can be reached by carefully controlling the quantity of the ammonia (solution 4), which depends on the Zn content. We measure the ammonia solution by a digital 100-1000 microliter pipet.

Our typical deposition conditions are:

(a) With Zn (20%-25%)

100 ml solution (1) + 100 ml solution (2) + 500 ml D.I. water + 2.0-2.4 ml solution (3)

Heat the mixture in the water bath to 82-85°C under constant stirring. Put the substrates into the solution and maintain the temperature. Chemical reaction starts after adding 160-200 microliter of solution (4). Duration of the deposition is 40 minutes. Thickness of the film is in the range 30-40 nm.

(b) Without Zn

20 ml solution (1) + 20 ml solution (2) + 660 ml D.I. water

Same temperature as above. Add 140-180 microliter of solution (4) to initiate the reaction. Film thickness is 30 to 35 nm. By changing the quantities of solution (1) and (2) to 30ml, water to 640 ml and solution (4) to 200 microliters, the film thickness increases to 35-45 nm.

Good films on glass should be visually shiny and uniform; and on selenide should be uniform with no powdery patches. After deposition, substrates should be rinsed well in D.I. water but no ultrasonic cleaning is necessary. Samples are subjected to a 5 minute bake in oxygen at 200°C immediately before the subsequent ZnO deposition process step.

2.3   ZnO Layer Deposition

The ZnO films are deposited in an inline system by RF magnetron sputtering onto the moving substrates in an argon or mixed oxygen and argon atmosphere. The most frequently used ZnO target is doped with 2% by weight of Al_2O_3. Two layers of ZnO film were deposited onto the thin sulfide covered selenide. The first high resistivity (≤ 10 ohm-cm) layer is approximately 50 nm thick. The second, low resistivity layer is approximately 300 nm in thickness and has a sheet resistivity of 25-65 ohm/square depending on the oxygen content in the sputtering atmosphere. As we dicussed before [3,4], the higher resistivity (65 ohm/square) is more transparent   than the lower resitivity (25 ohm/square) layer. Consequently, cell response is improved by using the higher resistivity film.

A ZnO target with 1% by weight of Al_2O_3 has been acquired and used during the last part of this work. The deposition charateristics are similar to the old 2% Al_2O_3 doped ZnO target. The resistivity is still highly sensitive to the oxygen content in the sputtering atmosphere. The optical properties of these films will be discussed in the section 3.2.

A second method for preparing the ZnO films has been developed which utilizes rotating cathode sputtering technology. This method offers considerable cost advantages for the film preparation in a manufacturing mode. In our approach, we have acquired a dual rotatable cathode module from Airco Coating Technology containing two 3" diameter Zn metal targets doped with Al (4 % atomic) and 16" in length. A cross sectional schematic is shown in Figure 2-1. Provisions were made to mount this module on the same inline vacuum system used to prepare the ZnO films by RF magnetron sputtering of a planar oxide target. A conceptual schematic of the CompTech system configured with the two sputtering type capabilities is depicted in figure 2-2. Figure 2-3 shows a typical installation arrangement for the cathode assembly on an inline vacuum system.
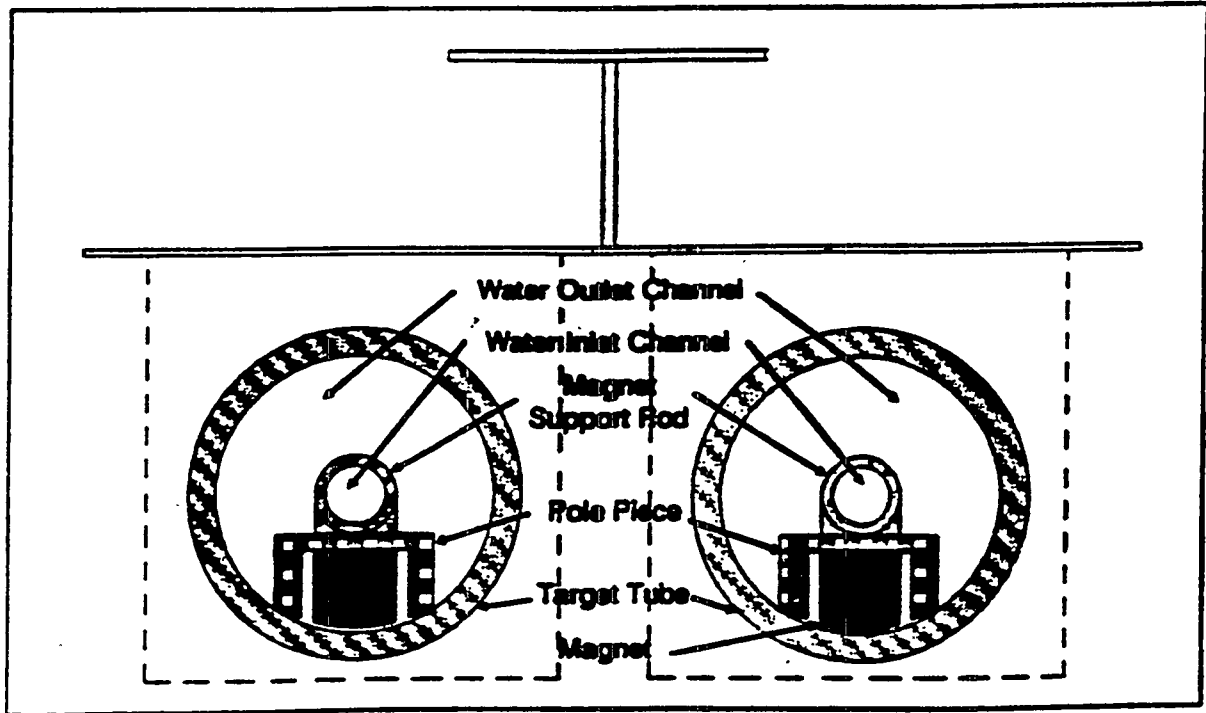
3

Figure 2–1. Dual rotatable cathode source cross-section
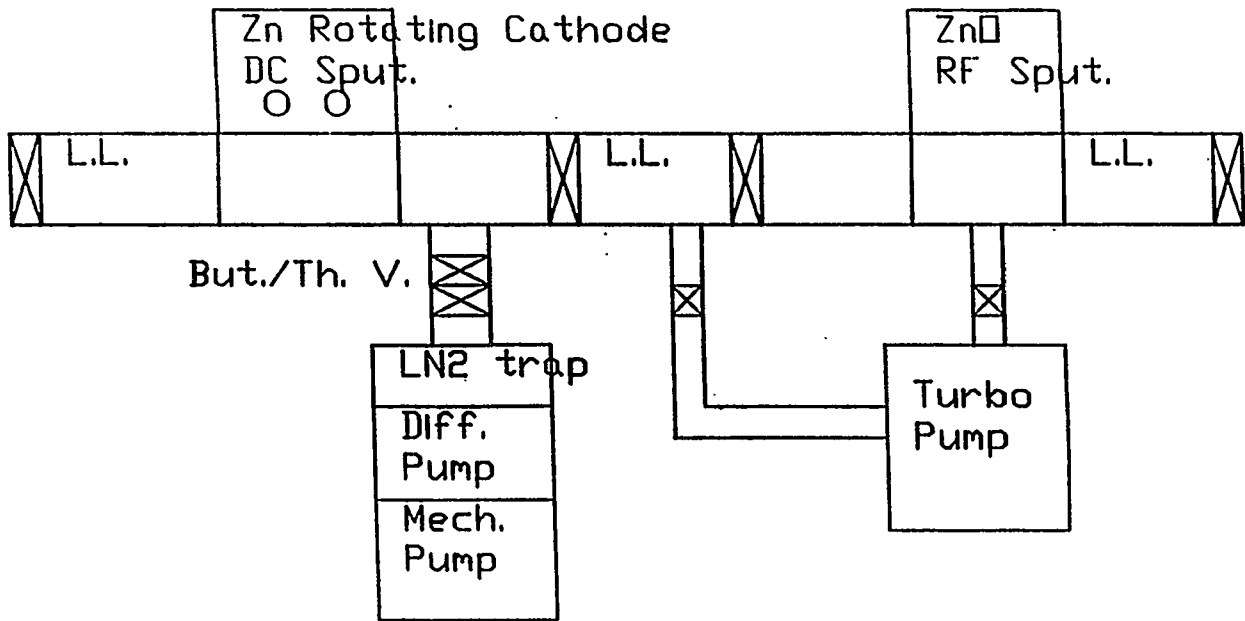
Figure 2–2. Schematic of CompTech inline deposition system

4
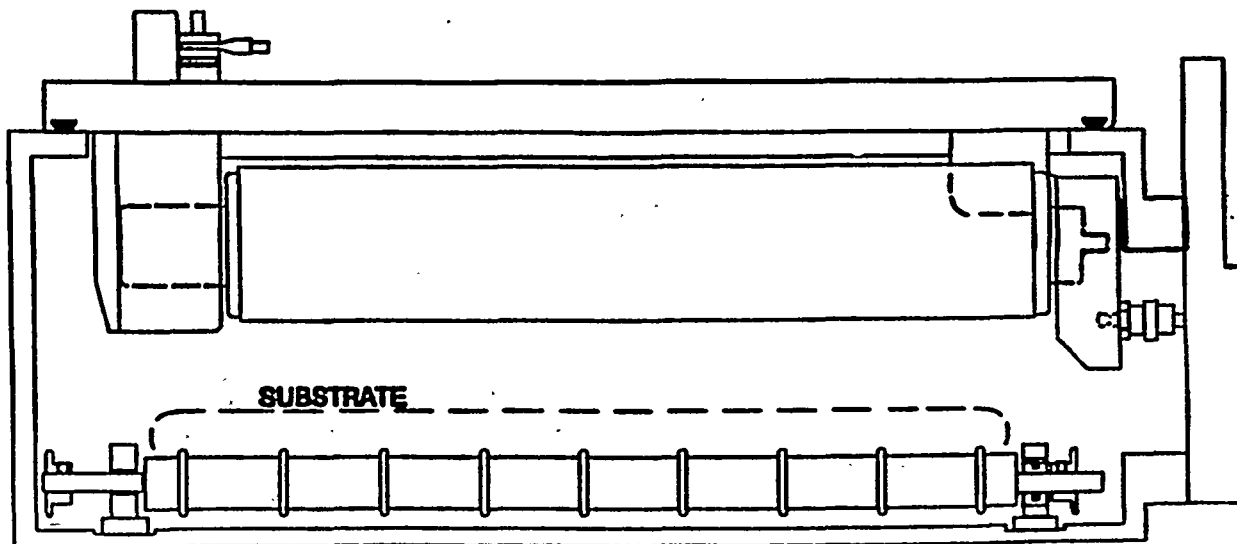
Figure 2–3.   ILS-1600 C-Mag® installation

The system commonality allowed use of the same mass flow gas controllers to introduce the Ar, Ar plus O_2, and O_2 sputtering gases. However, the two chamber zones (rotatable cathode and RF magnetron) are pumped by different means. A liquid nitrogen trapped diffusion pump equipped with an adjustable pumping restrictor is connected to the rotating cathode region while a turbopump exhausts the magnetron sputtering chamber. A MKS baratron gauge indicates pressures of approximately 5 millitorr during sputtering and a quadrupole mass spectrometer monitors the oxygen partial pressure before and after initiating the sputtering plasma. Substrates are loaded onto a 1 ft^2 pallet in a load lock chamber. The load lock is evacuated to less than 80 millitorr and then a slit valve opened to the sputtering chamber/module which is under high vacuum conditions ($< 3 \times 10^{-6}$ Torr). Using a track system, the pallet is passed below the cathodes until it is positioned in a "run out" chamber. While located within this chamber, the substrates are not in line of sight to the cathodes. The sputtering gases are introduced with the mass flow controllers in approximately a 5:1 flow rate ratio of Ar to O_2. The water cooled cathodes are rotated at 8-12 RPM. The two cathodes are electrically independent so that alloys or films with varying dopant levels and deposition rates may be prepared by suitable cathode material and/or power level selection. For the present experiments, only one cathode tube was connected to the DC power supply.

Once the gas pressures have stabilized, power is applied (1-1.2 kW) for about 5 minutes to precondition the cathode. The pallet conveyor system is then turned on and the pallets are transported beneath the cathodes at a controlled speed. By adjusting the track speed and number of passes, the film thickness can be controlled to achieve the desired sheet resistivity. For example, four passes produced a 1.1 micron thick film with a 40 ohm/square sheet resistivity. The deposition time was approximately one hour. The optical transmittance of this film, the beneficial effects of including H_2 with the sputtering gas, and other aspects of this advanced film deposition technique will be discussed in sections 3.2 and 3.3.

3.0   TECHNICAL DISCUSSIONS

3.1   CU(IN,GA)SE$_2$ FILM PREPARATION IMPROVEMENTS

As discussed in the Phase 1 Annual Report, several improvements had been incorporated into the CIGS film deposition equipment [4]. These improvements included a new substrate heater array and a rotating substrate holder that allowed deposition onto four 2" x 2" substrates each run. During this contract phase, we have expanded upon these features. Our primary goals were to maximize the film uniformity with respect to composition and morphology and to reduce the uncertainities relating to the actual temperatures of the rotating substrates.

Results on our fixed substrate CIS deposition system indicated a nonsymmetry in the deposited film appearance. This variation was not apparent in the EDS composition data, the SEM morphology pictures, or even in the cell performance measurements. However, it was clearly seen by simply viewing the substrates while they were rotated about an axis normal to the substrate plane.

The described variations were believed to be the result of using a single Se source located considerably off-axis to the substrate deposition area. This belief was confirmed by adding a second Se source on the opposite side of substrate area. The source sonsisted of a fused quartz crucible heated with a tungsten wire coil. The base of the crucible was clamped to a water cooled block to prevent thermal runaway due to the heat transfer from the high temperature substrates. Using with nearly equal flux rates from the two Se sources, no variations in the four 2" x 2" substrates at any viewing angle could be detected.

Although the CIGS system featured rotating substrates and should be less susceptable to the effects of Se source positioning, it was decided to install a second Se source to enhance uniformity in the deposition flux. In operation, the deposition rate of older source was typically set at 70-80% of its single source value while that of the added source provided a rate of about 30-40%.

The importance of substrate temperature to the CIGS film quality and cell performance was discussed in the Phase 1 report where only an apparent 30°C increase in temperature produced a substantial increase in grain size and cell efficiency. Measurements on multiple cells (4) formed on each 2" x 2" substrate and SEM morphology analysis indicated nonuniformities across the substrate area. The most likely origin for these gradients was thought to be temperature nonuniformities. In order to verify this assumption and to clarify questions concerning the absolute temperature values, a series of substrate temperature studies were conducted.

While thermocouples bonded to the substrate surface may normally be utilized to establish actual substrate temperature values and uniformites, this method is not very useful in the case of rotating sustrate systems. Instead, the approach taken was to deposit thin-film sandwich layers onto the substrate surface and observe transformations in these layers as the rotating substrate was heated. The materials selected for the sandwich were Ge and Au which have a 356°C eutectic at a composition of 12% Ge. Accordingly, test samples were prepared by depositing 100nm Ge films onto Mo metallized CMX glass substrates followed by 220 nm Au films. One test substrate and three standard Mo metallized glass substrates were loaded into the CIGS chamber substrate holder and some deposition shields removed so that the substrates could be observed as they were heated.

The most significant result from these tests was a severe nonuniformity in temperature as indicated by the film transformation patterns. A localized hot spot existed in the substrate region towards the center of the holder and generally coincided with one of the four 1 cm^2 cell areas. Outside the hot

6

spot region, the temperatures in the cell area appeared to be relatively uniform. This result would explain some of the cell performance data taken on cells from a single substrate. For example, the following table (3.1) lists data from one substrate (Mo metallized alumina, Run # 1516) which produced one of our highest efficiency devices.

Table 3-1. **Current-Voltage characteristics of four cells deposited onto an alumina substrate with an apparent temperature nonuniformity**

Cell	V_{oc} [V]	I_{sc} [mA]	FF	Efficiency[a] (%)
1516BA	0.5347	35.20	0.6691	12.59
1516BB	0.5231	36.36	0.6682	12.71
1516BC	0.5228	35.22	0.6847	12.61
1516BD	0.5440	35.73	0.6853	13.32

[a]Tests conducted at Boeing at 25°C, approximately 100 mW/cm^2, AM1.5G spectrum. All areas are assumed 1 cm^2.

The variation in cell performance with substrate position listed above is actually smaller than what we have typically observed. The key point is that one cell was nearly always superior and the other three were quite close to one another in performance. This superior cell was in the hot spot region on the substrate while the other three were in the lower, uniform temperature regions. Apparently, even the high thermal conductivity of alumina was not sufficient to smooth out the temperature gradients.

The preferred approach towards eliminating the gradients would have been to reposition the individual lamps in the substrate heater array but this is a very time consuming process and not compatible with our schedule. As an alternative, we increased the distance between the lamps and the substrates to the maximum extent possible with the existing tooling and we installed stainless steel foil shields to block part of the lamp illumination at the hot spot locations. By adjusting the size and position of the shields we were able to achieve satisfactory uniformity as indicated by the Ge/Au film transformation patterns on the glass substrates. Uniformity on alumina was anticipated to be even better due to the higher thermal conductivity.

The next deposition parameter to be addressed was that of the actual substrate temperature value. For these studies, calibration samples were prepared consisting of single crystal 2" diameter polished Si wafers which were coated with a 1 micron thick evaporated Al film. The wafers were then bonded to a Mo metallized alumina substrate using Sauereisen cement. The intent of the experiments was to use the 580°C Al/Si eutectic to calibrate the thermocouple probe contained in the deposition tooling which, in turn, controlled the power to the substrate heater. At the beginning of the experiments, the probe location was found to be providing poor correlation to the actual substrate temperature. Consequently, it was moved to a position between the lamps and substrates as close as possible (~3/8") to the back substrate surface. By making multiple runs with slight repositioning of the probe tip, agreement between the indicated probe temperature and the eutectic temperature was achieved. Since this temperature was in the range expected for the second CIGS film deposition, a reasonable correlation between indicated and actual film deposition temperatures was anticipated.

Deposition of CIGS films on Mo metallized alumina was then initiated using as target parameters a Cu/(In + Ga) ratio of 0.88-0.90, a Ga content of 24-27%, a first layer temperature of 450-480°C, and a second layer temperature of 550-580°C. According to the SEM analysis of films prepared with these parameters, the microstructure was very poor with a small average grain size in comparison with that of the 13% cell materials produced in the Phase 1 program. To improve this structure and subsequent cell efficiencies, the deposition temperatures were gradually increased for both CIGS layers and results monitored with the SEM. The final films were deposited at indicated temperatures of 660-695°C which was near the equipment limit. The films produced at these very high temperatures exhibited a microstructure similar to that of the previous high efficiency material but the grain size was still slightly smaller. We can only speculate that there were areas on the earlier nonuniformly heated substrates where temperatures possibly exceeded 700°C and thereby produced the localized, very high quality material. The I-V cell data for two alumina substrates deposited in a 660-680°C run are presented in table 3-2. Although the film composition slightly off the desired values (Cu/In + Ga) of 0.852 and Ga content of 26.6%, reasonable efficiencies and good cell uniformities were achieved. The highest efficiency device prepared in this recent study was deposited at indicated temperatures of 685-695°C. The I-V parameters for this device were V_{oc} of 0.5363 V, I_{sc} of 34.94 mA, FF of 0.6601, and efficiency of 12.37%.

Table 3-2. **Current-Voltage characteristics of eight cells deposited onto two alumina substrates following temperature nonuniformity corrections**

Cell	V_{oc} [V]	I_{sc} [mA]	FF	Efficiency[a] (%)
1564-1A	0.5063	33.56	0.6472	11.00
1564-1B	0.5109	33.33	0.6564	11.18
1564-1C	0.5104	33.54	0.6598	11.30
1564-1D	0.5060	34.05	0.6477	11.16
1564-2A	0.5113	34.74	0.6489	11.53
1564-2B	0.5082	34.62	0.6461	11.37
1564-2C	0.5061	34.49	0.6504	11.35
1564-2D	0.5102	35.03	0.6506	11.63

[a]Tests conducted at Boeing at 25°C, approximately 100 mW/cm^2, AM1.5G spectrum. All areas are assumed 1 cm^2.

The final CIGS film depositions made during the program were the result of suggestions by Lars Stolt and Jonas Hedström at the 23rd IEEE Phovoltaic Specialists Conference on use of soda lime glass substrates for CIGS cells [5]. For the glass substrate depositions, the substrate temperatures were lowered to 570-630°C. Alumina substrate were included for comparison purposes. The film compositions on the glass and alumina substrates were Cu/(In + Ga) of 0.887 and 0.906 and Ga concentrations of 24.6% and 26.8%, respectively. The strong influence of the substrate material with the high temperature depositions is shown in SEM photos of figure 3-1. The excellent microstructure of CIGS films on the soda lime glass is very evident in figure 3-1.a and resulted in our highest efficiency, highest voltage cells. Whether these very positive results are due to sodium, stress factors, or some other mechanism is unclear but this is certainly a promising area for future research.

8

a)   Soda-lime glass substrate
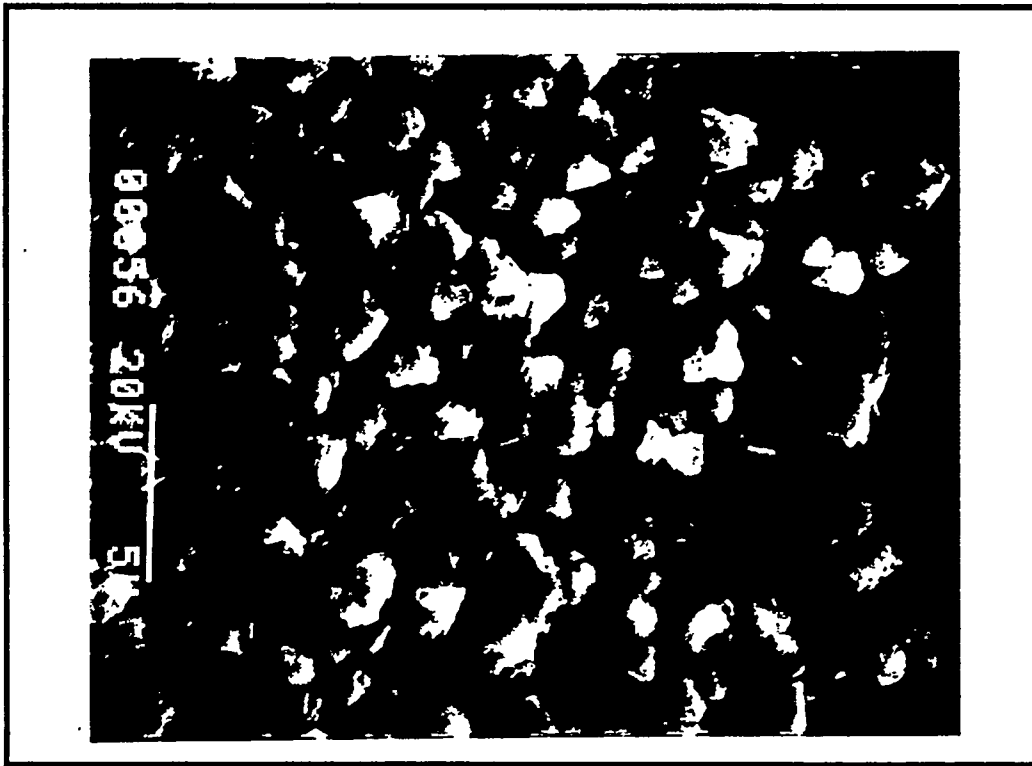
b)   Alumina substrate

Figure 3–1.   SEM photographs of CuInGaSe$_2$ simultaneously grown on
                      soda lime glass (a) and alumina (b) substrates.

9

3.2 OPTICAL PROPERTIES OF ZnO FILMS

Optical properties, transmittance and reflectance, of ZnO films sputtered form targets doped with 1% and 2% of Al_2O_3 and reactive sputtered from Zn metal rotating target doped with 4 atm% of Al, were measured on a Perkin-Elmer Lambda-9 spectrophotometer. The transmittance plus reflectance curves of these films are shown in figure 3.2 as a function of wavelength. The first curve (I) is the transmission property of the film sputtered from ZnO target doped with 1% Al_2O_3. The film had sheet resistivity of 50 ohm/square and thickness of approximately 300 nm. The second curve (II) is for a film from the target with 2% Al_2O_3, which had a resistivity of 54 ohm/square and was about the same thickness as the film of the first curve. Both films have excellent transmission up to wavelengths of 850 nm. The roll-off at the longer wavelengths due to the free carrier absorption is reasonable for both films. The film from the target with 1% Al doping has less free carrier absorption as compared to the film from the target with higher Al doping. This indicates that lowering the Al doping improves the electron mobility in the films. The third curve (III) represents the property for the film sputtered from the rotating metal target, with sheet resistivity of 40 ohm/square and thickness of 1.1 micrometers. The inferior property of this film as compared to the properties of the previous two films could indicate that the sputtering process has yet to be optimized and/or due to excessively high doping of this target.
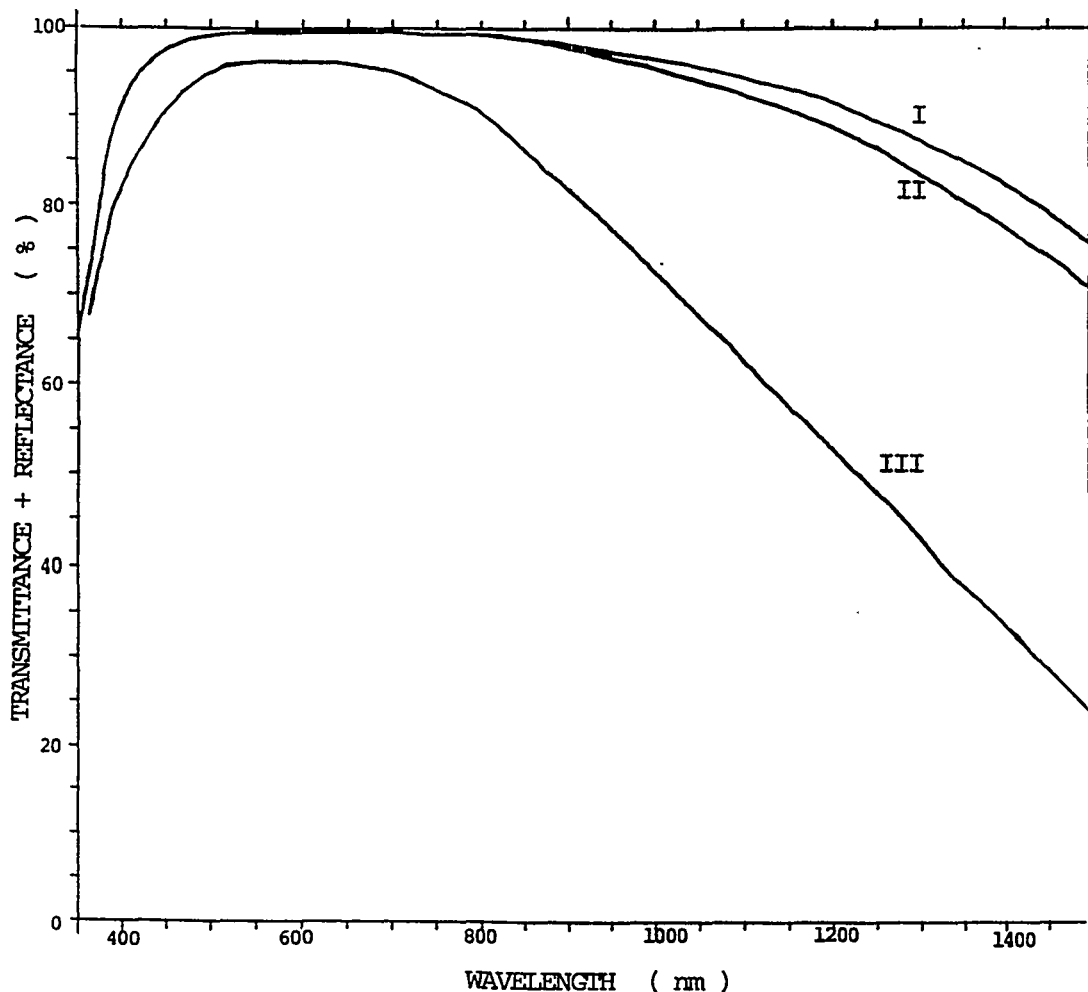

Figure 3–2.   Optical properties of sputtered ZnO films.

3.3   ZnO Films Prepared by Rotating Cathode Sputtering

Because of cost considerations, the deposition of films using rotating cathode sputtering is an extremely important techology. Accordingly, during Phase 2 we have explored the application of this technology to the preparation of the transparent, conductive ZnO films. A description of the deposition equipment and general process is given in Section 2.3.

In order to establish this process, we conducted ZnO film depositions as a function of O_2 flow rates, Ar to O_2 flow ratios, total chamber pressure, DC power levels, track speed, cathode rotation rate, etc. The resulting films were characterized for transparency, sheet resistance, and thickness. As in other reactive sputtering systems, the most important parameters were the oxygen flow rate and the applied power level. There were basically two competing oxidation processes occurring during the deposition process. One was the oxidation of the deposited film on the substrate while the other was the oxidation of the Zn metal cathode. A higher oxygen flow rate favors cathode oxidation resulting in low cathode voltages, a low film deposition rate, high optical transparency, but low conductivity even with the Al dopant. According to residual gas analyzer, the oxygen partial pressure decreases by only about 20% from the value before the discharge is initiated. Lower oxygen flow rates result in a metallic cathode characteristics with high voltages, high deposition rates, and conductive but dark films. The oxygen partial pressure is reduced to around 20-30% of the pre-discharge value. To prepare films with both high transparency and conductivity requires intermediate oxygen flow rates. Unfortunately, in this region the discharge becomes unstable and may switch with time between the two states (oxide or metal target surface). This troublesome problem is described in detail in the references [6,7,8]. The solution has been to apply sophisticated target/chamber configurations, very high pumping speeds, or feed-back control systems between the oxygen flow rate and the metal emission rate. These techniques were not available to us for the present program. By carefully monitoring the deposition parameters of voltage, oxygen partial pressure, and total chamber pressure, 300 nm thick films of good transparency with 1200 ohm/square sheet resistivity could be prepared in a single 20 minute pass under the cathode. The stability and reproducibility of the discharge were so poor, however, that multiple passes to increase the film thickness and reduce the sheet resistance were not possible. This situation only changed when we replaced the pure Ar sputtering gas with a mixture of Ar/5% H_2. It now appeared that we could successfully operate in the stable, oxidized cathode region but still produce electrically conductive films. Instead of extreme sensitivity to oxygen flow rate or applied power, these parameters could easily and controllably be varied without causing major changes to the discharge or film properties. Although the deposition rate was low, the process stability permitted multiple passes and with four passes a 40 ohm/square film was prepared. Other deposition parameters for this film have been discussed in section 2.3. The optical transparency is depicted in figure 3-2 along with RF sputtered ZnO films. The data indicates improvements to the process will be needed to match the quality of the RF sputtered films but these early results on production-oriented process are very encouraging.

11

3.4 CHARACTERISTICS AND ANALYSIS OF CELLS

In the last annual report of this work, we reported our first cell with an AM1.5 total area efficiency over 13% [4]. That cell (1490AD) had V_{oc}=0.5184 volt, J_{sc}=34.80 mA/cm^2, fill factor =72.82%, and efficiency =13.1% as measured at NREL. The selenide of that cell had mole fraction of gallium, [Ga]/([In]+[Ga]), of 0.20. The lower gallium content results in a lower V_{oc}. The reasons for the significant improvement in the cell fill factor are the high quality, dense thin sulfide films and high quality selenide film obtained by depositing at higher substrate temperatures.

Detailed loss analysis has been performed on a similar cell from the same substrate of that cell [4,9]. Those results are summarized in table 3-3.

Table 3-3. **The effect on efficiency of removing the major quantified loss mechanisms in the best Phase 1 cells, as determined for cell #1490AC.**

Loss mechanism	Relative power gain
Reflection (not AR coated)	+5.0%
Grid shadowing losses	+2.2%
ZnO Optical Losses:	
Wavelength independent absorption:	+4.5%
ZnO bandedge	+1.7%
IR absorption (free carrier)	+1.8%
CdZnS absorption(no ZnO)	+1.8%
Selenide IR rolloff	+2.4%
ZnO sheet resistance loss[a]	+0.3%
Grid resistance losses[a]	+1.4%

[a]calculated

These results indicate that cell performance could be significantly improved by reducing the reflection loss and ZnO absorption losses. Applying a simple quarter wave AR coating of MgF$_2$ has been tested to provided a 2-3% improvement of current. To reduce the ZnO absorptions, higher sheet resistivity material (~60 ohm/square) which has better transmission charateristics than the lower resistivity material, can be used.

Cells were fabricated with the above improvements and with the selenide gallium content increased from 20% to 26% during the second phase of this work. The I-V charateristics of our best 1 cm^2 cell grown on alumina (1516BD) is shown in figure 3-3. The cell is seen have V_{oc}=0.5458 volt, J_{sc}=36.71 mA/cm^2, fill factor=68.38% and efficiency=13.7%.

The Cu, Ga, In, and Se composition in atomic percentages of the best cell was 23.38, 6.99, 19.70, and 49.93, respectively. The mole fraction of Ga was 0.262. A plot of the relative quantum efficiency versus wavelength of the cell measured by NREL is shown in figure 3-4. In the same figure, the best cell is compared to the cell with 13.1% efficiency. The long wavelength absorption edge is shifted approximately 0.042 eV towards shorter wavelengths due to the higher Ga content of the best cell. A comparison of the two cells indicates a V_{oc} increase of 0.0274 volts when the Ga content increased form 0.20 to 0.26. Accordingly, the V_{oc} increase is seen to be slightly less than 2/3 of the bandgap change.

Boeing, ZnO/CdZnS/CIGS/Mo/Al Global

Sample: 1516BD   Temperature = 25.0°C

Jul. 1, 1992 10:56 am   Area = 0.9895 cm²
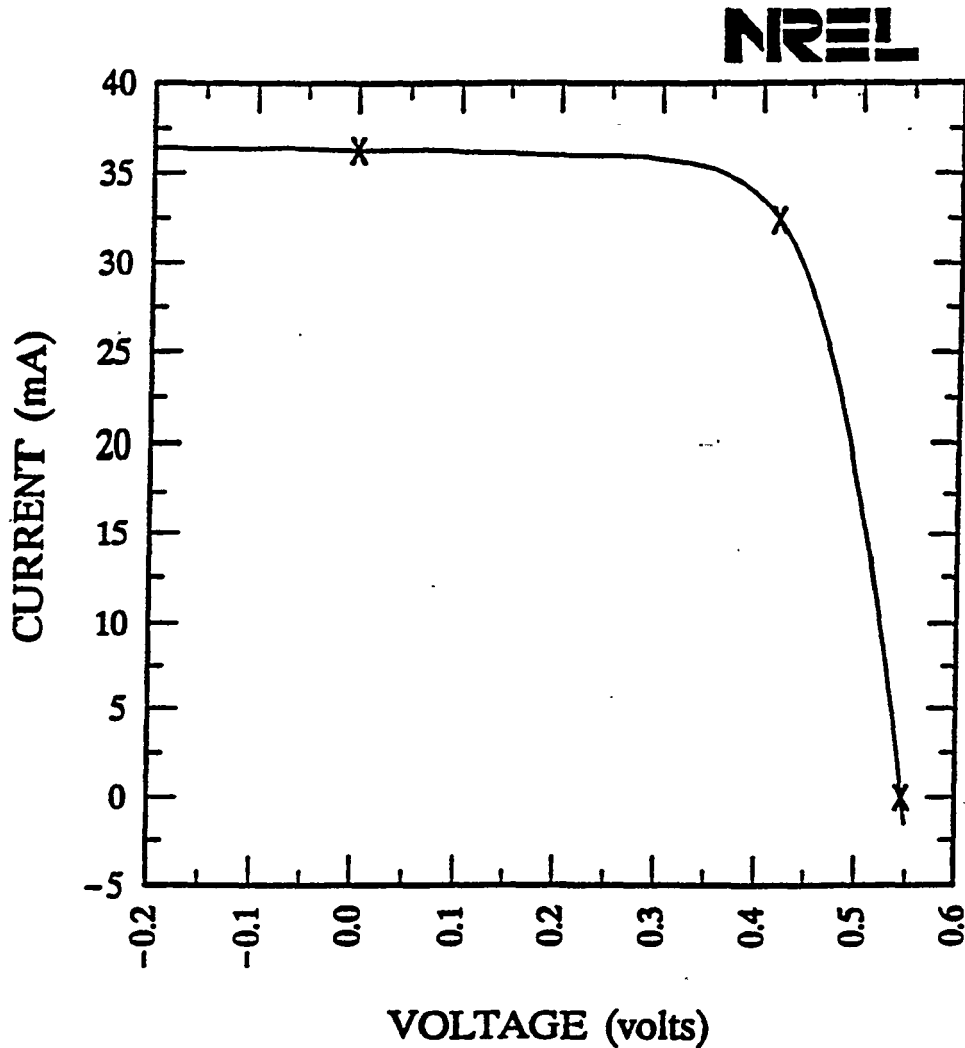
NREL

V_{oc} = 0.5458 volts I_{sc} = 36.34 mA

J_{sc} = 36.71 mA/cm² P_{max} = 13.56 mW

Fill factor = 68.38 % I_{max} = 32.44 mA

Efficiency = 13.7 % V_{max} = 0.4181 V

Figure 3–3.   I-V characteristics of best CuInGaSe₂ cell on alumina as measured by NREL.
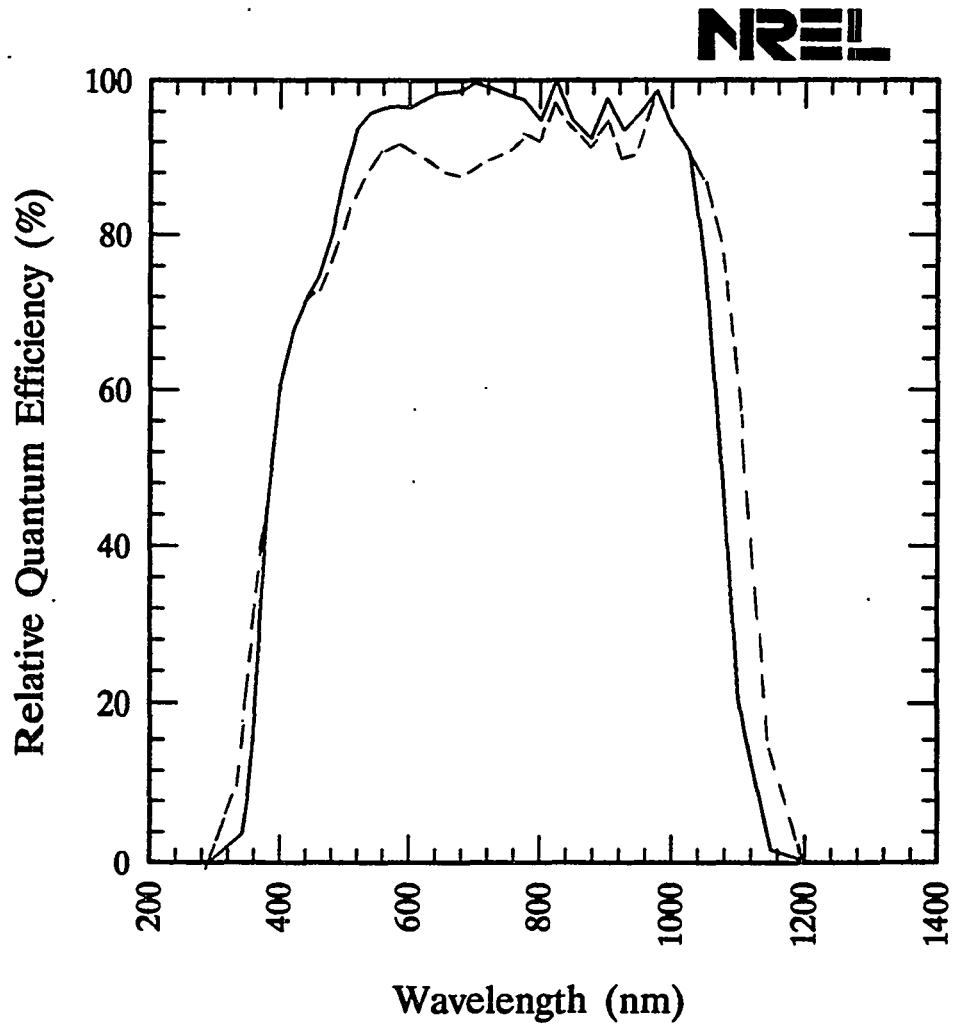
13

Boeing, ZnO/CdZnS/CIGS/Mo/Al

Sample: 1516BD   Temperature = 25.0°C

Jun. 30, 1992 12:06 pm   Area used = 0.9895 cm²

NREL

Light bias = 5.00 mA

Zero voltage bias

Figure 3–4.   Relative quantum efficiency of cell 1490AD (dashed line) and 1516BD (solid line) as measured by NREL.

14

The reduction of fill factor of the cell 1516BD can not be attributed to the higher resisitivity ZnO layer. According to our calculation, the fill factor should only decrease by less than 0.6% with the change of ZnO sheet resistivity from 30-60 ohm/square. The major cause of the reduction could be due to the use of deposition conditions which have not yet been optimized for the preparation of high quality selenide material with high gallium content.

In spite of possessing a higher bandgap, cell 1516BD actually displays a more than 5% higher short circuit current than cell 1490AD. Part of the increase is due to the application of a MgF_2 AR coating and part is due to using a ZnO film with less optical losses.

One means of demonstrably improving the quality of selenide material with high gallium content is to utilize soda lime glass substrates rather than alumina, as discussed in section 3.1. The cell data as measured at Boeing from the best substrate fabricated during our limited experiments using soda lime glass are listed in table 3-4, and the NREL-measured I-V curve and QE curve for the best of these cells are shown in figures 3-5 and 3-6 respectively.

Table 3-4.   Current-Voltage characteristics of four $CuIn_{.75}Ga_{.25}Se_2$ cells deposited onto a soda lime glass substrate

Cell	V_{oc} [V]	I_{sc} [mA]	FF	Efficiency[a] (%)
1570-4A	0.5840	35.25	0.6901	14.20
1570-4B	0.5824	35.74	0.6825	14.20
1570-4C	0.5801	35.48	0.6911	14.23
1570-4D	0.5790	34.97	0.6867	13.90

[a]Tests conducted at Boeing at 25°C, approximately 100 mW/cm^2, AM1.5G spectrum. All areas are assumed 1 cm^2.

Boeing CIGS

Sample: 1570-4/A

Aug 25, 1993 4:11 PM

Spectrum: ASTM E892-87 Global

Temperature = 25.0°C

Area = 0.9954 cm^2

Irradiance: 1000.0 Wm^{-2}
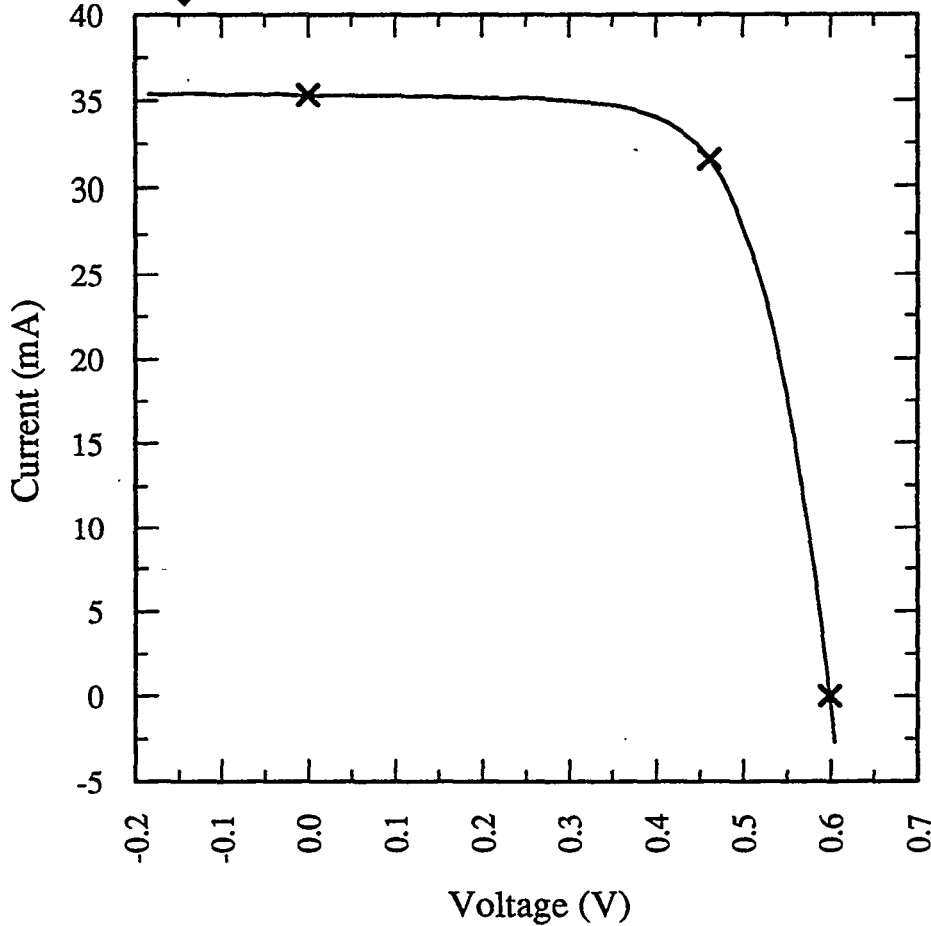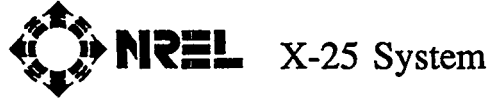
NREL X-25 System

V_{oc} = 0.5996 V

I_{sc} = 35.32 mA

J_{sc} = 35.48 mAcm^{-2}

Fill Factor = 68.82 %

V_{max} = 0.4618 V

I_{max} = 31.56 mA

P_{max} = 14.57 mW

Efficiency = 14.6 %

Figure 3–5.   **I-V characteristics of best CuInGaSe$_2$ cell *on soda lime glass* as measured by NREL.**

Boeing CIGS

NR

Light bias = 5.00 mA

Zero voltage bias

Figure 3-6.   Relative quantum efficiency of best CuInGaSe$_2$ cell *on soda lime glass* as measured by NREL.

4.0 CONCLUSIONS

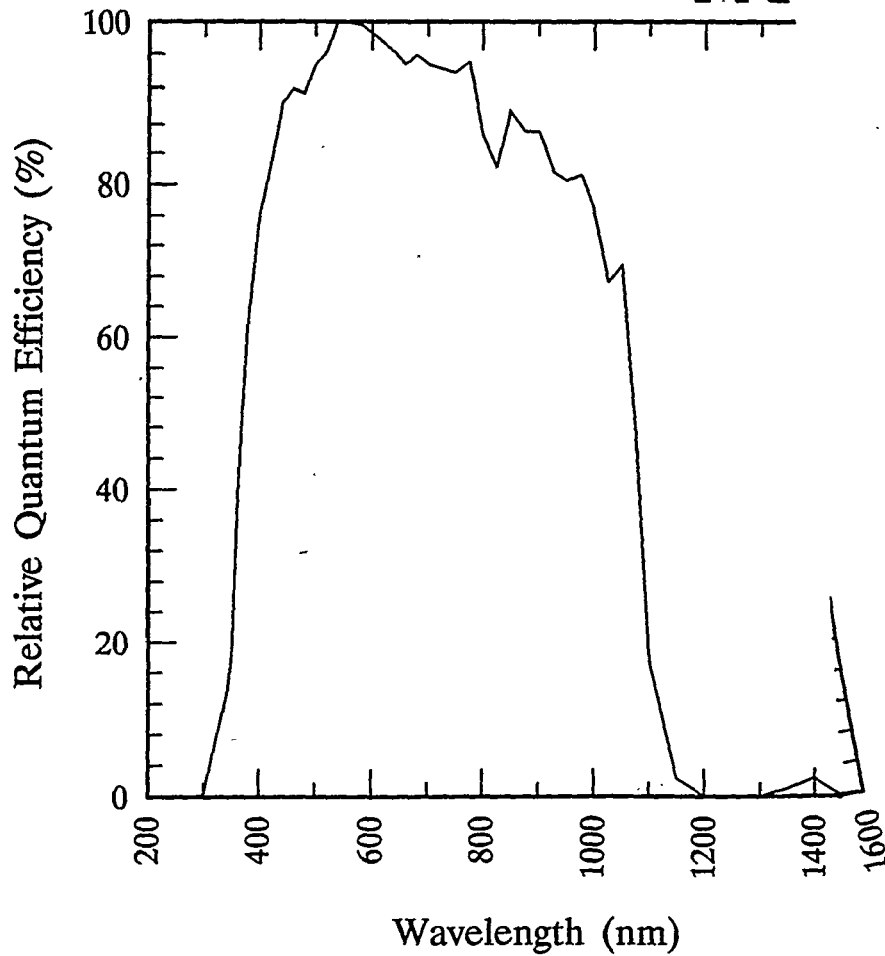The value of using a detailed loss analysis on prior cells as a guide for cell improvement has been clearly demonstrated. The major optical losses of reflection and ZnO absorption were identified and addressed in the fabrication of subsequent CIGS cells on alumina substrates and resulted in a maximum total area efficiency for a CIGS cell on alumina of 13.7%. In addition to reduced optical losses, the quality of the CIGS material was improved by increasing the film deposition temperature.

Substrate temperature calibration tests using eutectic formation temperatures for thin-film structures on Mo metallized glass and Si wafers indicated that deposition temperatures for this highest efficiency CIGS material on alumina could have exceeded 700°C in localized substrate areas.

The thin-film eutectic samples were found to be extremely useful in analyzing temperature nonuniformities in rotating substrate deposition systems. The improved uniformity resulting from these studies was demonstrated by a much less scatter in the performance values of multiple cells prepared on a single substrate.

Although the difference was small (a few percent), the long wavelength transmittance of ZnO films prepared by RF magnetron sputtering from ZnO targets doped with Al_2O_3 was higher when the dopant level was reduced from 2% to 1% (by weight).

Feasibility of using rotating cathode sputtering as a low cost production method for ZnO films has been demonstrated by the preparation of 1.1 micron thick films with 95% transmittance and 40 ohm/square sheet resistance using a Zn metal target doped with Al (4% atomic) and Ar/O_2 sputtering gas mixtures. Use of 5% H_2 in the Ar was found to greatly stabilize the reactive sputtering process and made that approach successful.

CIGS films deposited onto Mo metallized soda lime glass substrates exhibited a far superior microstructure to those deposited onto Mo metallized alumina even when they were prepared at a lower substrate temperature (630°C vs. 695°C). The films were more dense and possessed a larger grain size. The improved morphology was reflected in cell performance, and devices exceeding 580 mV open circuit voltage with over 14% total area efficiency were produced.

5.0 REFERENCES

1. W.S. Chen, J.M. Stewart, B.J. Stanbery, W.E. Devaney, and R.A. Mickelsen, "Development of Thin Film Polycrystalline $CuIn_{(1-x)}Ga_xSe_2$ Solar Cells", The Conference Record of the 19th IEEE Photovoltaic Specialists Conference, 1987, pp. 1445-1447.

2. W.E. Devaney, W.S. Chen and J.M. Stewart, "High Efficiency $CuInSe_2$ and $CuGaInSe_2$ Based Cell and Materials Research", Final Technical Progress Report, Contract ZL-8-06031-8, May, 1990.

3. W.E. Devaney, W.S. Chen, J.M. Stewart and R.A. Mickelsen, "Structure and Properties of High Efficiency $ZnO/CdZnS/CuGaInSe_2$ Solar Cells", IEEE Trans. Electron Device, Vol. 37, 428, (1990).

4. B.J. Stanbery, W.S. Chen, W.E. Devaney, and J.M. Stewart, "Research on Polycrystalline Thin-Film $CuGaInSe_2$ Solar Cells", Annual Subcontract Report, Contract ZH-1-19019-6, November, 1992.

5. Jonas Hedström, Håkan Ohlsén, Marika Bodegård, Angela Kylner, Lars Stolt, Dimitri Hariskos, Martin Ruckh, and Hans-Werner Schock, "$ZnO/CdS/Cu(In,Ga)Se_2$ Thin Film Solar Cells with Improved Performance", to be published in The Conference Record of the 23rd IEEE Photovoltaic Specialists Conference, May, 1993.

6. M.J. Brett and R.R. Parsons, "Stoichiometry control mechanisms for bias-sputtered zinc-oxide films", Can. J. Phys. 63, 819, (1985).

7. S. Berg, H.O. Blom, M. Moradi, and C. Nender, "Process modeling of reactive sputtering", J. Vac. Sci. Technol. A 7, 1225 (1989).

8. R.P. Howson, A.G. Spencer, K. Oka, and R.W. Lewin, "The formation and control of direct current magnetron discharges for the high-rate reactive processing of thin films", J. Vac. Sci. Technol. A 7, 1230 (1989).

9. W.E. Devaney, W.S. Chen, J.M. Stewart and B.J. Stanbery, "Analysis of High Efficiency $CuGaInSe_2$ Cells", Conf. Proc. of PVAR&D, Denver, CO, 1992, AIP Conf. Proc. 268, Ed. R. Noufi, 1992, p.157.

APPENDIX A

THIN FILM CuInGaSe$_2$ CELL DEVELOPMENT

Wen S. Chen, J.M. Stewart, W.E. Devaney, R.A. Mickelsen and B.J. Stanbery

Boeing Defense and Space Group

Seattle, Washington 98124

ABSTRACT

The characteristics of polycrystalline, thin film CuIn$_{1-x}$Ga$_x$Se$_2$ (CIGS)/ZnO solar cells with a total area efficiency of 13.7% are reported. These nominally 1 cm^2 cells are prepared by elemental coevaporation of the selenide material, chemical deposition of a thin (20-30 nm) CdZnS layer and RF magnetron sputtering of the ZnO transparent conductive film. The Ga and Zn contents were measured to be 26% and 20%, respectively. We attribute the improved performance over our previous CIGS cells to a slightly higher Ga concentration and to the preparation of ZnO films with lower optical losses.

INTRODUCTION

The use of the ternary chalcopyrite compound CuInSe$_2$ as the p-type base absorber layer in a heterojunction solar cell with CdS or CdZnS as the n-type window layer has been well established [1]-[3]. The rationale for replacing the ternary CuInSe$_2$ with its quaternary analog Cu(In,Ga)Se$_2$ has also been discussed [4]-[6]. This work is a continuation of our research to develop thin film polycrystalline heteroface solar cells using CIGS as the p-type absorber layer, CdZnS mixed alloys as the n-type layer, and a n-type overlayer of ZnO transparent conducting oxide for majority carrier collection. Our best prior cell was a 1 cm^2 ZnO/CdZnS/CuInGaSe$_2$ cell with an AM1.5 total area efficiency of 12.5% [6]. In this paper the charateristics of CIGS cells with a total area efficiency over 13% are reported and discussed.

CELL STRUCTURE AND PREPARATION

The cross sectional structure of the present cells is shown in Figure 1. This is essentially unchanged from the previous work [6]. Our bilayer CuIn$_{1-x}$Ga$_x$Se$_2$ films are prepared by multisource simultaneous elemental deposition onto heated molybdenum-coated alumina substrates. The substrate temperature ranges from 450-500°C for the first, Cu-rich layer and 500-550°C for the second, Cu-poor layer. The substrate temperature has
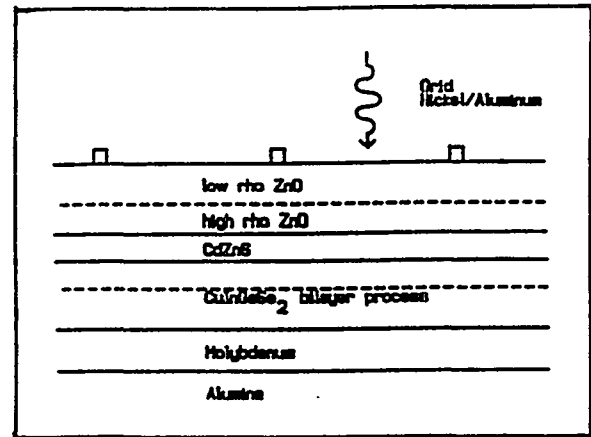

Figure 1. Cross section of ZnO/CdZnS/CuInGaSe$_2$ cell. The layers are not to scale.

a significant effect on the film composition as well as morphology [7]. CIGS films with a composition of Cu/(In+Ga)=0.89 and X=27% and deposited at a final substrate temperature of 500°C have a grain size on the order of one micron or less. The grains of CIGS films with similar compositions may be increased to the order of 5 microns by only increasing the final deposition temperature to 530°C. During the early period of our work, CIGS films were deposited with a final substrate temperature up to 500°C. These films yielded devices in the range of 12% in efficiency. Efficiencies in excess of 13%, which have been exhibited by our more recent devices, have been partly due to an improved CIGS grain structure resulting from an increase in the substrate temperature beyond 500°C. Careful control of the substrate temperature and temperature-time profile have also been found important for run to run reproducibility. While our chemical bath deposition of ultra-thin sulfide thin films has been described previously [6], a number of process refinements have now been incorporated. Solutions of CdCl$_2$, ZnCl$_2$ and thiourea are pre-mixed and the solution is continually stirred as it is brought to a temperature of 80-90°C. After a proper amount of NH$_4$OH is added, substrates

are then immersed into the solution. The reaction in the solution goes to completion in approximately 30-40 minutes during which time deposition of a film of 20-30 nm thickness occurs. Without the addition of Zn, good quality uniform sulfide films are easily made. However, good films containing Zn can only be made by tightly control the amount of NH_4OH in the solution The transparent, conductive ZnO overlay films are deposited onto the moving substrates in an inline vacuum system by RF magnetron sputtering with an argon or mixed oxygen and argon atmosphere. The details of the deposition process were described in references [6] and [8]. In the cell structure, the high resistivity (~10 Ohm-cm) ZnO layer is approximately 50 nm thick. The low resistivity layer with thickness of approximately 300 nm has a sheet resistivity of 25-65 Ohm/square depending on the oxygen content in the sputtering atmosphere. The lower resistivity (25 Ohm/square) material is less transparent than the higher resistivity (65 Ohm/square) material. The grid structure for the top electrode is formed by vacuum deposition through a metal stencil mask. Aluminum is used as the main grid material while a nickel film serves as a contact layer between the aluminum and the ZnO.

CELL CHARACTERISTICS AND ANALYSIS

Figure 2 shows the I-V characteristics of our first cell (1490AD) with an AM1.5 total area efficiency over 13%. This cell had V_{OC}=0.5184 volt, J_{SC}=34.80 mA/cm^2, fill factor=72.82%, and efficiency= 13.1% as measured at the National Renewable Energy Laboratory (NREL). The quantum efficiency (QE) of this same cell as measured in our laboratory is shown in Figure 3. The
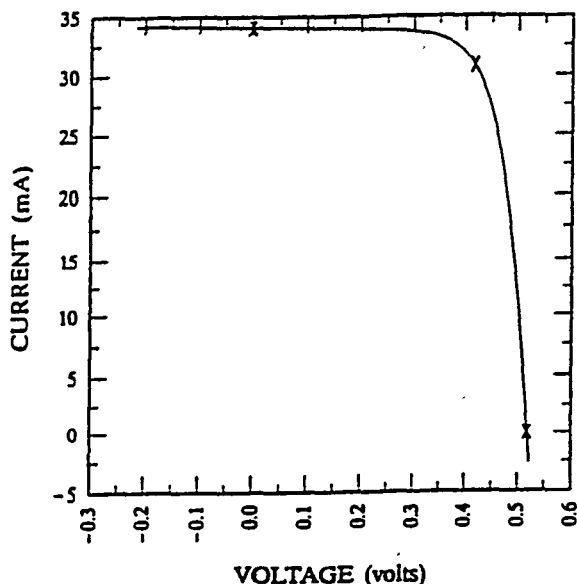

Figure 2. I-V characteristics of cell 1490AD as measured at NREL. V_{OC}=0.518 volts, I_{SC}=34.1 mA, ff=0.728, Eff.=13.1%. Cell area 0.979 cm^2.
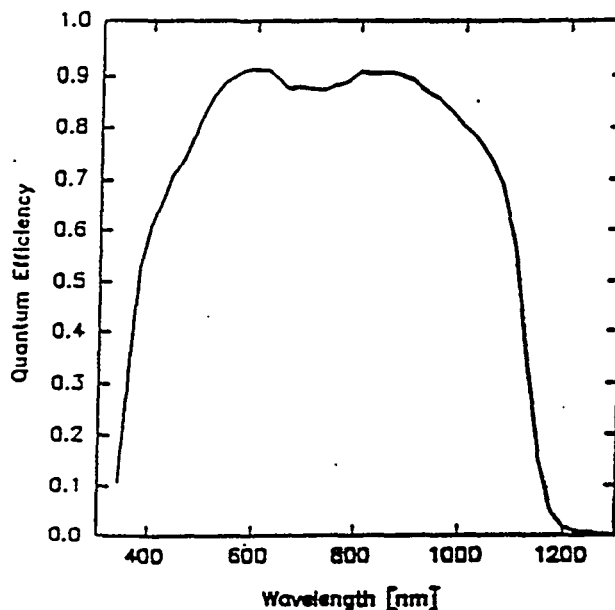

Figure 3. Quantum efficiency of cell 1490AD with 20% Ga.

measurement was at short circuit bias and was found to be independent of any applied light bias.

The selenide of this cell had a overall composition of 23.4, 21.2, 5.4, and 50.0 in atomic percent as mesured using EDX for Cu, In, Ga, and Se, respectively . The mole fraction of Ga, i.e., [Ga]/([In]+[Ga]), is calculated to be 0.20. This value is considerably lower than the 0.28 used in the previous best cell [6]. The lower Ga content results in a lower V_{OC} but a most significant improvement in the cell fill factor. One of the major reasons for the improvement is an absence of local shunting defects which have been present in the majority of earlier cells. These defects have been due to an inferior quality, e.g., porous and nonuniform, thin sulfide layer. By refining the chemical dipping process as discussed above, high quality dense thin sulfide films can now be reproducibly made. This has resulted in the reduced shunting observed in the newer cells. However, shunt improvement alone is not sufficient to explain all of the increase in fill factor. Improved selenide film quality, as obtained by depositing at higher substrate temperatures, is believed to be another important factor.

Detailed analysis has been performed on a similar cell from the same substrate of 1490AD [7][8]. Major losses were identified and quantified from the experimental results. Table I shows a summary of the losses in the cell as expressed by the fractional increase available in I_{SC} if the loss was reduced to zero.

21

LOSS MECHANISM	RELATIVE GAIN
Reflection (non-AR coated)	5.0%
Grid Shadowing Losses	2.2%
ZnO Optical Losses:	
Wavelength independent absorption	4.5%
ZnO bandedge	-1.7%
IR absorption (free carrier)	1.8%
CdZnS Absorption (no ZnO)	1.8%
Selenide IR Rolloff	2.4%
ZnO Sheet Resistance Loss	0.3%
Grid Resistance Losses	1.4%

TABLE I. The effect on efficiency of removing the major quantified loss mecanisms in cell 1490AC.

The analytical results shown in Table I quantify several clear paths to further efficiency improvement. Significant improvement can be made by reducing the cell reflection loss and ZnO absorption losses. The simplest method for reducing the reflection losses in the cell is to apply a quarter wave coating of MgF_2. This prediction has been tested and shown to provided a 2-3% improvement in current [7]. Because ZnO sheet resistance losses are so low, higher sheet resistance material (~60 Ohm/square), which has better transmission characteristics than the 25 Ohm/sqaure material, can be used.

Cells were fabricated with the above improvements implemented and with the selenide Ga content increased from 20% to 26%. The I-V characteristics measured by NREL of our resulting best 1 cm^2 cell (1516BD) is shown in Figure 4. The cell is seen have $V_{oc}=0.5458$ volt. $J_{sc}=36.71$ mA/cm^2, fill factor=68.38% and efficiency=13.7%. This is the highest reported total area efficiency for a CIS based thin film solar cell.

The Cu, Ga, In, and Se composition in atomic percentages of the best cell was 23.38, 6.99, 19.70, and 49.93, respectively. The mole fraction of Ga was 0.262. A plot of the quantum efficiency versus the wavelength of the cell is shown in Figure 5. In the same figure, the best cell is compared to the cell 1490AD. The long wavelength absorption edge is shifted approximately 0.42 eV due to the higher Ga content of the best cell. A comparison of the two cells indicates a V_{oc} increase of 0.274 volts when the Ga content increased from 0.20 to 0.26. Accordingly, the Voc increase is seen to be slightly less than 2/3 of the bandgap change.

In spite of possessing a higher bandgap, cell 1516BD actually displays a more than 5% higher short circuit current than cell 1490AD. Part of the increase is due to the application of a MgF_2 antireflection coating and part is due to using a ZnO film with higher resistivity ZnO but lower optical absorption and scattering.
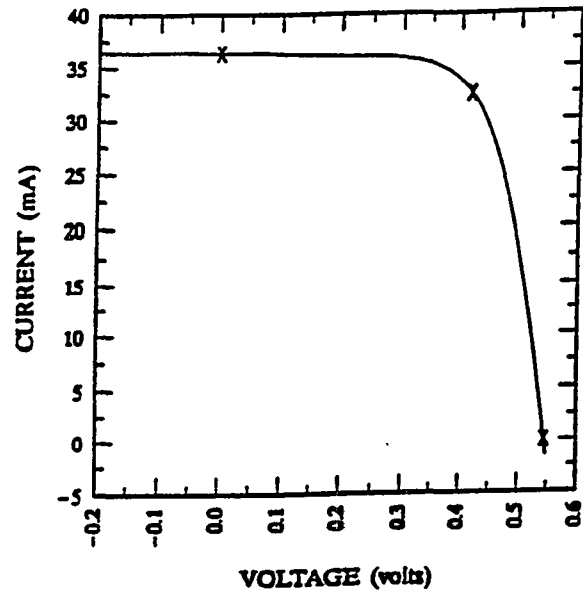

Figure 4. I-V characteristics of cell 1516BD as measured at NREL. $V_{oc}=0.546$ volts, $I_{sc}=36.3$ mA, ff=0.684, Eff.=13.7%. Cell area 0.9895 cm^2.
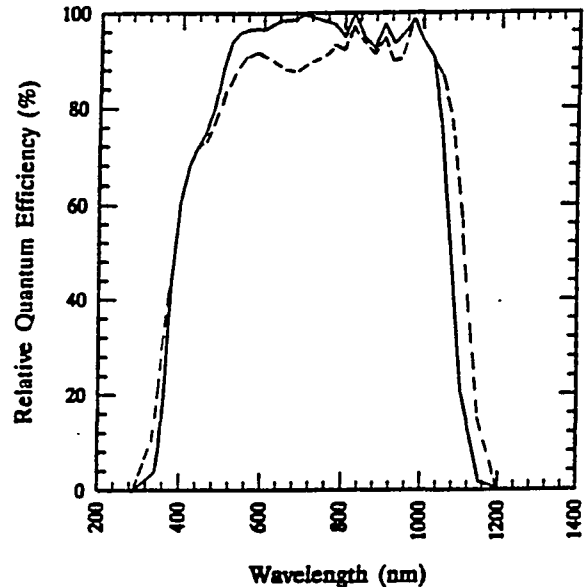

Figure 5. Relative Quantum efficiencies of cell 1490AD (dashed line) and 1516BD (solid line) as measured at NREL.

The reduction of fill factor of the cell 1516BD can not be attributed to the higher resistivity ZnO layer. According to our calculation, the fill factor should only decrease by less than 0.6% with the change of ZnO sheet resistivity from 30 to 60 Ohm/square. The major cause of the reduction could be due to the use of deposition conditions which have not yet been optimized for the preparation of high quality selenide material with high Ga content.

SUMMARY AND CONCLUSION

We have made significant improvements in the performance of $ZnO/CdZnS/CuInGaSe_2$ thin film cells. Efficiencies have increased, for example, to 13.7% from a previously reported value of 12.5%.

In general, the improvements are attributed to a better selenide grain structure resulting from a higher substrate temperature during deposition and to a better quality CdZnS film achieved by refining the chemical dipping process. In particular, we have analyzed the material properties and cell performance of a cellency and have identified the loss mechanisms. By reducing the reflection loss, reducing the ZnO absorption losses, and increasing the Ga content in the selenide, we made the highest reported total area efficiency of 13.7% for a CIS based thin film solar cell. With the optimization of selenide deposition parameters to restore the fill factor loss in the best cell, we are confident that cells with a total area efficiency well above 14% could be developed.

REFERENCES

[1] K. Zweibel, "Photovoltaic Cells", *Chem. & Eng. News*, p.34, July, 7 ,1986.

[2] R. A. Mickelsen, W. S. Chen, B. J. Stanbery, and W. E. Devaney, "Polycrystalline $CuInSe_2$ Thin-Film Solar Cells", *Proc. int. 3rd PVSEC* (Tokyo, Japan), 1987.

[3] J. Ermer, C. Fredric, K. Pauls, D. Pier, K. W. Mitchell, and C. Eberspacher, "Recent Progress in Large Area $CuInSe_2$ Submodules", *Proc. int. 4th PVSEC* (Sydney, Austrlia), 1989.

[4] J. M. Stewart, W. S. Chen, W. E. Devaney and R. A. Mickelsen, "Thin Film Polycrystalline $CuIn_{1-x}Ga_xSe_2$ Solar Cells", *Proc. 7th Int. Conf. Ternary and Multinary Compounds*, Sept., 1986, Eds. S. K. Deb and A. Zunger, Material Research Society, 1987.

[5] W. S. Chen, J. M. Stewart, B. J. Stanbery, W. E. Devaney, and R. A. Mickelsen, "Development of Thin Film Polycrystalline $CuIn_{1-x}Ga_xSe_2$ Solar Cells", *Proc. 19th IEEE PVSC*, 1987, p.1445.

[6] W. E. Devaney, W. S. Chen, J. M. Stewart and R. A. Mickelsen, "Structure and Properties of High Efficiency $ZnO/CdZnS/CuInGaSe_2$ Solar Cells", *IEEE Trans. Electron Devices*, Vol.37, No.2, 1990, p428.

[7] B. J. Stanbery, W. S. Chen, W. E. Devaney and J. M. Stewart, "Research on Polycrystalline Thin Film $CuInGaSe_2$ Solar Cells", *Phase I Annual Technical Progress Report*, May 3, 1991-May 2, 1992, NREL Substract No. ZH-1-19019-6, May, 1992.

[8] W. E. Devaney, W. S. Chen, J. M. Stewart and B. J. Stanbery,"Analysis of High Efficiency $CuInGaSe_2$ Based Solar Cells", Photovoltaic Advanced Research and Development Project, Denver, CO., 1992, *AIP Conf. Proc. 268*, Ed. Rommel Noufi, 1992, p.157.

ABSTRACT

The objectives of this research effort were to fabricate high efficiency $CdZnS/CuGaInSe_2$ thin film solar cells, and to develop improved transparent conductor window layers such as ZnO.

Better yield, uniformity and reduced shunting resulted from improvement of our CBD process for deposition of ultrathin CdZnS films.

Continuous improvement of our baseline RF magnetron sputtering process gave the best TCO (combining high conductivity and long wavelength transmittance) with films from ZnO targets doped with 1% Al_2O_3 (by weight). Rotating cathode sputtering was demonstrated as an alternative lower cost production method using a Zn metal target alloyed with Al (4% atomic) and an Ar/O_2 sputtering gas mixture. Addition of H_2 stabilized this reactive DC magnetron sputtering process.

CIGS films deposited onto molybdenum-metallized soda lime glass substrates were more dense and possessed a larger grain size than those deposited onto molybdenum-metallized alumina. Substrate thermal uniformity was essential to reducing performance variability across each substrate.

Combining these material, equipment and process improvements enabled the fabrication of four $\cong 1cm^2$ $ZnO/Cd_{0.76}Zn_{0.24}S/CuIn_{0.75}Ga_{0.25}Se_2$ cells on a single low-cost soda lime glass substrate with mean $V_{oc} = 0.581$ volts, $I_{sc} = 35.36$ mA, FF = 0.687 and *total* area cell efficiency (with standard deviation) of **14.13±0.13%** AM1.5G.

Document Control Page	1. NREL Report No. NREL/TP-413-5835	2. NTIS Accession No. DE94000203	3. Recipient's Accession No.

4. Title and Subtitle

Research on Polycrystalline Thin Film CuInGaSe$_2$

5. Publication Date

October 1993

6.

7. Author(s)

W.S. Chen, J.M. Stewart, R.A. Mickelsen, W.E. Devaney, B.J. Stanbery

8. Performing Organization Rept. No.

9. Performing Organization Name and Address

Boeing Defense & Space Group
P.O. Box 3999, M/S 9E-XX
Seattle, WA 98124=2499

10. Project/Task/Work Unit No.

PV331101

11. Contract (C) or Grant (G) No.

(C) ZH-1-19019-6

(G)

12. Sponsoring Organization Name and Address

National Renewable Energy Laboratory
1617 Cole Blvd.
Golden, CO 80401-3393

13. Type of Report & Period Covered

Technical Report
3 May 1991 - 21 May 1993

14.

15. Supplementary Notes
NREL technical monitor: H.S. Ullal

16. Abstract (Limit: 200 words)

This report describes work to fabricate high-efficiency CdZnS/CuInGaSe$_2$ thin-film solar cells and to develop improved transparent conductor window layers such as ZnO. The specific technical milestone for Phase I was to demonstrate an air mass (AM) 1.5 global 13%, 1-cm^2 total-area CuInGaSe$_2$ (CIGS) thin-film solar cell. For Phase II, the objective was to demonstate an AM1.5 global 13.5%, 1-cm^2 total-area efficiency. We focused our activities on three areas. First, we modified the CIGS deposition system to double its substrate capacity. Second, we developed new tooling to enable investigation of a modified aqueous CdZnS process in which the goal was to improve the yield of this critical step in the device fabrication process. Third, we upgraded the ZnO sputtering system to improve its reliability and reproducibility. A dual rotatable cathode metallic source was installed, and the sputtering parameters were further optimized to improve ZnO's properties as a transparent conducting oxide (TCO). Combining the refined CdZnS process with CIGS from the newly fixtured deposition system enable us to fabricate and deliver a ZnO/Cd$_{0.80}$Zn$_{0.20}$S/CuIn$_{0.74}$Ga$_{0.26}$Se$_2$ cell on alumina with I-V characteristics, as measured by NREL under standard test conditions, of 13.7% efficiency with V_{oc} = 0.5458 V, J_{sc} = 35.48 mA/cm^2, FF = 0.688, and efficiency = 14.6%.

17. Document Analysis
  a. Descriptors
    polycrystalline ; thin film ; photovoltaics ; solar cells

  b. Identifiers/Open-Ended Terms

  c. UC Categories
    273

18. Availability Statement
  National Technical Information Service
  U.S. Department of Commerce
  5285 Port Royal Road
  Springfield, VA 22161

19. No. of Pages

31

20. Price

A03